

THZ OPTICAL PROPERTIES OF A LARGE QUANTUM DOT-DOUBLE RING IN EXTERNAL FIELDS

Doina BEJAN¹, Cristina STAN^{2*}

We present a theoretical study on the response in the electronic and optical properties of a large experimental structure of a GaAs/GaAlAs quantum dot – double ring subjected to external electric and magnetic fields. The energy and optical absorption spectra are also considered for the case of laser dressed structure, for different values of laser parameters. Our results revealed that the energy of the experimental structure is strongly influenced by the electric or magnetic fields but much less by the intense laser field. We obtained specific characteristics in energy and optical properties that can be useful in experimental applications.

Keywords: quantum dot-double quantum ring, electric field, magnetic field, laser dressed parameters

1. Introduction

Theoretical studies on semiconductor quantum structure evolve in a rapid way due to the continuous need of new technological applications in optoelectronic devices, bioimaging and biosensing, security systems, advanced quantum computing and information processing, environmental and chemical sensing, nanoelectronics spintronics, etc [1,2]. Experimental study of quantum nanostructures involves a lot of sophisticated fabrication and characterization techniques, such as Molecular Beam Epitaxy, Metal-Organic Chemical, Vapor Deposition or Self-Assembly Techniques including Stranski-Krastanov Growth or Colloidal Synthesis [3-5].

An efficient way to control the electronic and optical responses of semiconductor structures can be achieved by external fields: either electric or magnetic

¹ Assoc. Prof., Faculty of Physics, University of Bucharest, Bucharest, Romania, e-mail: doinita.bejan@unibuc.ro

^{2*} Prof., Faculty of Applied Sciences, UNSTPB, Bucharest, Romania, e-mail: cristina.stan@upb.ro

or both [6-18]. Also, a high intensity laser field can deform the confining potential without inducing any change in the physical structure, allowing a good control of energy spectrum and optical properties [19-22].

In our previous papers [23,24] we performed systematic analysis of quantum dot-double ring (QDDR) nanostructures of small dimensions with the in-plane diameter restricted up to 60nm, based on the experimental cross- sectional profile given in [5]. This type of structures has been experimentally fabricated and studied since 2011 by Somaschini group [5]. They showed that it is possible to couple, within a single structure, systems with different dimensionalities (dots and rings), in close spatial proximity. Such nanostructures exhibit strong photoluminescence and large design flexibility.

In this study we choose to examine how constant electric and magnetic fields influence the electronic and optical properties of large structures, given that the experimental QDDR described in [5] has a substantial diameter of approximately 360 nm. The investigations involve 3D numerical computations, based on the effective mass approximation.

The paper is organized as follows. In Section 2 we describe the theoretical framework for QDDR in the presence of electric, magnetic and intense laser fields. The electronic and optical properties are presented and analyzed in Section 3. Finally, the conclusions are summarized in Section 4.

2. Theory

The height profile is obtained from the fitting of the mediated right and left parts of the experimental cross-sectional profile given by [5].

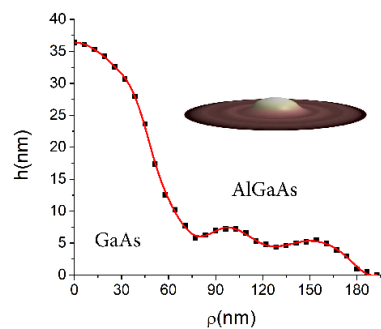


Fig.1 Mediated right and left profiles (squares) of experimental QDDR [5] and the fitted function (curve). Inset is the 3D reconstruction of QDDR built by revolving the profile around the z-axis.

The electron confining potential $V_c(x, y, z)$ and the effective mass of the electron $m^*(x, y, z)$ confined in the QDDR made of GaAs/Al_{0.3}Ga_{0.7}As can be written using the Heaviside step function H as follows:

$$\begin{aligned} V_c(x, y, z) &= V_0 (H(-z) + H(z - h(\rho))) \\ m^*(x, y, z) &= m^*_{GaAs} + (m^*_{AlGaAs} - m^*_{GaAs}) (H(-z) + H(z - h(\rho))) \end{aligned} \quad (2)$$

where $\rho = \sqrt{x^2 + y^2}$, V_0 is the barrier potential for electrons in GaAs/Ga_{0.7}Al_{0.3}As and $h(\rho)$ is the height profile constructed as a superposition of three Gaussian functions as described in [23].

We consider in our computation three different external applied fields:

- (a) an intense laser radiation taken as a monochromatic field linearly polarized on x direction, described by the potential vector of amplitude A_{0L} and angular frequency ω_L : $\vec{A}_L(t) = \hat{x}A_{0L} \cos(\omega_L t)$;
- a) a static axial magnetic field $\vec{B} = B\hat{z}$ derived from the potential vector $\vec{A}_m = B/2(-y, x, 0)$ as $\vec{B} = \nabla \times \vec{A}_m$.
- b) a static electric field acting along x -axis, $\vec{F} = \hat{x}F$.

Here, \hat{x} and \hat{z} are the unit vectors along the x and z axes, respectively;

In the presence of all external fields, the electron motion is described by the solution of the time-independent Schrödinger equation obtained after performing the Kramers-Henneberger unitary transformation [25]:

$$\left(-\frac{\hbar^2}{2} \nabla \left(\frac{1}{m^*(x, y, z)} \nabla \right) + V_{cd}(x, y, z, a) + U_{md}(x, y, a) + exF \right) \Psi(x, y, z) = E\Psi(x, y, z) \quad (3)$$

where the dressed potentials are:

$$V_{cd}(x, y, z, a) = \frac{\omega_L}{2\pi} \int_0^{2\pi/\omega_L} V_c(x + a \cos(\omega_L t), y, z) dt \quad (4)$$

and

$$U_{md}(x, y, a) = \frac{e^2 B^2}{8m^*} \left(x^2 + \frac{a^2}{2} + y^2 \right) + \frac{ieB}{2m^*} \left(y \frac{\partial}{\partial x} - x \frac{\partial}{\partial y} \right) \quad (5)$$

The value a is the laser-dressing parameter defined as [21]:

$$a(x, y) = \frac{eA_{0L}}{m^*\omega_L} \quad (6)$$

is a measure of the ILF irradiation and is position dependent through the effective mass. The lower limit for application of the dressing model for quantum structures is in THz frequency range.

The energy eigenvalues E and eigenfunctions $\Phi(x, y, z)$ were calculated numerically using FEM (Finite Element Method) as incorporated by COMSOL Multiphysics® software [26]. The spatial domain of integration has a cylindrical shape, coaxial with the QDDR, with height and radius twice the structure dimensions. In the computation we use an adaptative free tetrahedral mesh with Dirichlet conditions for the boundary of the cylindrical domain. More technical details on the FEM 3D mesh can be found in [21,27].

To describe the absorption of the large QDDR, we make use of the Paspalakis *et al.* [28] approximation for the susceptibility induced by a probe laser obtaining the following equation for the absorption coefficient:

$$\alpha_{ij}(\omega) = \frac{Ne^2 \mu_{ij}^2 T_2}{\varepsilon_0 \hbar c n_r} \frac{\left| J_0^2 \left(\frac{|\mu_{jj} - \mu_{ii}| e E_0}{\hbar \omega} \right) - J_2^2 \left(\frac{|\mu_{jj} - \mu_{ii}| e E_0}{\hbar \omega} \right) \right|}{1 + T_2^2 (\omega - \omega_{ji})^2 + \bar{\mu}_{12}^2 E_0^2 T_1 T_2 / \hbar^2} \quad (7)$$

where ω is the angular frequency and E_0 the amplitude of the electric field of the probe, $\omega_{ji} = \frac{E_j - E_i}{\hbar}$, J_0, J_2 are the first kind Bessel functions of order 0 and 2, T_1 is the population decay time and T_2 the dephasing time, ε_0 is the vacuum permittivity. Also,

$$\bar{\mu}_{ij} = \mu_{ij} \left(J_0 \left(\frac{|\mu_{jj} - \mu_{ii}| e E_0}{\hbar \omega} \right) + J_2 \left(\frac{|\mu_{jj} - \mu_{ii}| e E_0}{\hbar \omega} \right) \right) \quad (8)$$

where the electric dipole matrix elements for a probe laser polarized along the x -axis are specifically defined as:

$$\mu_{ij} = \langle \Psi_i(x, y) | x | \Psi_j(x, y) \rangle. \quad (9)$$

3. Results and discussion

The following numerical values are used in our computations: the effective mass of the electron in GaAs is $m_{*_{GaAs}} = 0.067 \cdot m_0$ while in AlGaAs is $m_{*_{GaAlAs}} = 0.0919 \cdot m_0$ where m_0 is the mass of a free electron, e -electron charge and $V_0 = 262$ meV for GaAs/Ga_{0.7}Al_{0.3}As). Other values are: $N = 5 \times 10^{22} \text{ m}^{-3}$, $n_r = 3.55$, $T_1 = 10 \text{ ps}$, $T_2 = 5 \text{ ps}$ [24] and laser probe irradiation of 10^7 W/m^2 .

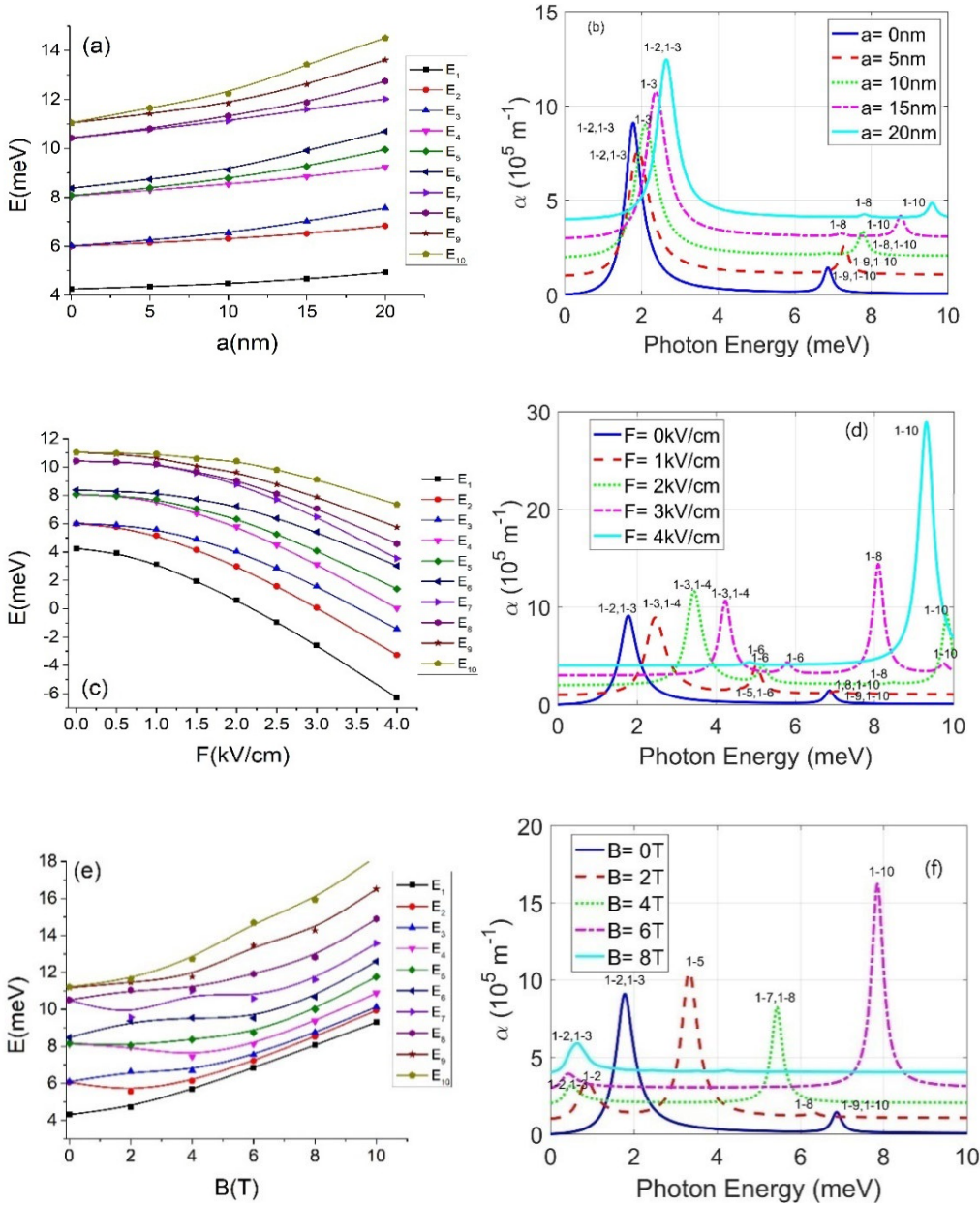


Fig.2 Energy spectra (first column) and optical absorption (second column) for the variation of: laser dressed parameter: (a), (b), electric field (c), (d), and magnetic field (e), (f).

Figure 2 show the QDDR responses to the three considered external fields. We consider in our computation the first ten energy levels.

We firstly analyze the electronic response represented by the energy spectra illustrated in Fig.2 (a), (c), (e). As is seen, in the absence of any external fields, many excited levels come into pairs.

In the case of the laser dressing control (Fig.2(a)), the energy levels remain paired for $a=0-5\text{nm}$ and are negligibly increased. A significant increment and distinct separation of the levels are observed starting with $a>10\text{nm}$.

The largest sensibility of QDDR energy spectra is detected for the static electric field (Fig.2(b)). The energy levels separation is already achieved starting with $F=1\text{kV/cm}$. The levels decrement in energy as electric field is augmented shows a quadratic Stark effect up to $F=2\text{kV/cm}$ then follows a linear trend.

For the case of magnetic field control (Fig.2(e)), the ground level just increases quadratically with the field, analogously to the diamagnetic shift in quantum dots and quantum wells [21] since the wave-function of the ground state is located only on the dot. The energy levels of the excited states display some oscillations (Aharonov-Bohm like), although they are not well defined, as the wave-functions of the excited states penetrate only slightly in the rings.

A useful tool in the analysis of the electronic response is the average location on x axis for the electron in the ground state (actually the dipole moment μ_{11}) for the three cases of external field control given in Table 1.

Table 1

The values of the average position of electron in the ground state

$\langle x_1 \rangle [\text{nm}]$					
$a[\text{nm}]$		$F[\text{kV/cm}]$	$B[\text{T}]$		
0	0.02605	0	0.026051	0	0.02605
5	0.01544	1	20.53626	2	0.11315
10	0.31622	2	29.92812	4	0.11306
15	0.12646	3	33.62494	6	0.01984
20	0.02602	4	36.38028	8	0.08913

In the first two columns, it is observed that the deformation of the structure as the result of the asymmetry induced on x axis by the laser dressing, changes slightly the electron location, without any clear dependence. Since the magnetic field is along z -axis, the localization of electron can be a little increased/decreased (last two columns) but these small variations are negligibly small in comparison with the total width of the structure (360nm). As expected, the location control is better achieved using an electric field, the electrons being pushed stronger from the dot to the inner or even to the outer ring as the value of F increases.

The optical response is represented by the absorption spectra displayed in Figs.2(b), (d), (f), which are computed with Eq. (7), considering the transitions from state 1 to the excited states 2-10. The specific maxima location and their values are determined by the competition between the values of the transition energy and dipole transition moments.

The values of dipole moments for the main transitions involved in optical spectra are given in Table 2.

Table 2

The dipole moments values in (nm) for the significant transitions

	(1-2)	(1-3)	(1-4)	(1-5)	(1-6)	(1-7)	(1-8)	(1-9)	(1-10)
$a=0$	14.5688	5.7334						1.1788	0.8178
$a=5$	1.3600	15.0231						0.1858	1.4702
$a=10$		14.4333					0.3415		1.3147
$a=15$		13.5307					0.4456		1.1489
$a=20$	0.3489	12.7087			0.1857		0.4657		0.9345
--	--	--	--	--	--	--	--	--	--
$F=1$		12.9679	0.8523		2.5684		0.4951		0.3538
$F=2$		9.6815	1.9459		0.2597		0.4192		3.0085
$F=3$		5.7756	1.4568		4.6848		0.9804		6.2799
$F=4$		0.8087	0.2275		9.0690		2.6412	0.2378	7.8985
--	--	--	--	--	--	--	--	--	--
$B=2$	10.0648		0.7036	9.7173			0.7051		
$B=4$	7.8977	0.1724			0.25194	4.0250			
$B=6$	7.3201	0.2890	0.2291				0.1567		5.4459
$B=8$	6.3556	0.9793	0.4802	0.2905	0.10635	0.27776	0.1815		

In the absence of external fields, the allowed transitions are 1-2, 1-3 at around 2meV with high intensity due to the large transition moments and 1-9, 1-10 at around 7meV with a low intensity since the involved moments are much lower. This is observed in the first blue curve on each case of the absorption graphs of Fig.2. However, each external field has a specific effect on this characteristic absorption of the unperturbed QDDR.

Figure 2(b) show that the intense laser displaces slightly the absorption peaks to higher energies, due to the faster increment of the energies of the excited states in comparison with the increment of the ground state as seen in Fig.2(a). The electric field (Fig.2(c)) has a different impact, leading to a higher blue-shift of the peaks due to the faster decrement of the ground level energy. It is also observed that new peaks are involved in the absorption spectra. One can notice the large 1-10 peak that appears at 4kV/cm owing to the large deformations of the wave-functions in the field presence. For the case of magnetic field (Fig.2(c)), it can be seen a decrement of peaks maxima and a weak oscillatory behavior of the peaks location due to the oscillations appearing in the energy spectrum.

4. Conclusions

In this paper, we presented theoretical studies on the effects of external electric, magnetic and intense laser fields on an experimental quantum dot-double ring structure.

Our results revealed that, for a large QDDR structure, the intense laser has a low influence on the energy and absorption spectra. On the contrary, these spectra are strongly modified by rather low values of the static electric field or by the magnetic field. The laser and the static electric fields induce only blue-shifts of the absorption peaks but the magnetic field lead to blue or red-shifts depending on the value of the field. Therefore, the optical properties can be controlled efficiently and tuned in the range of specific practical interest, using the electric and magnetic fields.

R E F E R E N C E S

- [1] *T. Chakraborty*, Nanoscale Quantum Materials: Musings on the Ultra-Small World, *CRC Press, Taylor-Francis Group*, 2021.
- [2] *V. Fomin*, Physics of Quantum Rings, 2nd ed., Springer-Verlag, Berlin Heidelberg, 2014.
- [3] *A. D. Yoffe*, Semiconductor Quantum Dots and Related Systems: Electronic, Optical, Luminescence and Related Properties of Low Dimensional Systems, *Adv. in Phys.* **50** (2001) 1-208.
- [4] *C. Somaschini, S. Bietti, A. Fedorov, N. Koguchi and S. Sanguinetti*, Concentric multiple rings by droplet epitaxy: fabrication and study of the morphological anisotropy. *Nanoscale Res. Lett.* **5** (2010) 1865.
- [5] *C. Somaschini, S. Bietti, A. Fedorov, N. Koguchi and S. Sanguinetti*, Coupled quantum dot-ring structures by droplet epitaxy, *Nanotechnology* **22** (2011) 185602.
- [6] *D. Bejan, C. Stan*, Oscillatory behaviour in the energy and nonlinear optical rectificationspectra of elliptic quantum rings under electric field: influence of impurity and eccentricity, *Philos. Mag.* **99** (2019) 492.
- [7] *G. Rezaei, N. A. Doostimotlagh*, External electric field, hydrostatic pressure and conduction band non-parabolicity effects on the binding energy and the diamagnetic susceptibility of hydrogenic impurity quantum dot, *Physica E* **44** (2012) 833.
- [8] *D. Bejan, C. Stan, O. Toma*, Magnetic field controlled induced transparency by Autler-Townessplitting in pseudo-elliptic quantum ring, *Eur. Phys. J. B* **92** (2019) 153.
- [9] *D.A Ospina, D. Duque, M. E. Mora-Ramos, et al.* Hopf-link GaAs-AlGaAs quantum ring under geometric and external field settings, *Physica E* **163** (2024) 116032.
- [10] *J. A. Vinasco, A. Radu, E. N. Niculescu, et al.* Electronic states in GaAs-(Al, Ga)As eccentric quantum rings under nonresonant intense laser and magnetic fields. *Sci. Rep.* **9**(2019) 1427.
- [11] *E. Acosta, A. L. Morales, C. M. Duque, M. E. Mora-Ramos, C. A. Duque*, Optical absorption and refractive index changes in a semiconductor quantum ring: Electric field and donor impurity effects, *Phys. Status Solidi B* **253** (2016) 744.
- [12] *J.I. Clemente and J. Planelles*, Characteristic molecular properties of one-electron double quantum rings under magnetic fields, *J. Phys. Condens. Matter* **20** (2008)035212.
- [13] *D. Bejan, C. Stan, A. Petrescu-Niță*, Magnetic properties of pseudo-elliptic quantum rings: influence of impurity position and electron spin, *U.P.B. Sci. Bull., Series A* **84** (2022) 163.
- [14] *D. Bejan, C. Stan*, Geometry tailored magneto-optical absorption spectra of elliptically deformed double quantum rings. *Philos. Mag.* **102** (2022) 1755.
- [15] *J. Planelles, F. Rajadell and J.I. Clemente*, Electron states in quantum rings with structural distortions under axial or in-plane magnetic fields. *Nanotechnology* **18** (2007) 375402.
- [16] *D. Bejan, C. Stan*, Influence of spin-orbit interaction, Zeeman effect and light polarisation on the electronic and optical properties of pseudo-elliptic quantum rings under magnetic field, *Philos. Mag.* **100** (2020) 749.
- [17] *D. Bejan, C. Stan*, Electron spin and donor impurity effects on the absorption spectra of pseudo-elliptic quantum rings under magnetic field, *Philos. Mag.* **101** (2021) 1871.
- [18] *F.J. Culchac, N. Porras-Montenegro and A. Latgé*, GaAs-(Ga,Al)As double quantum rings: confinement and magnetic field effects. *J. Phys. Condens. Matter* **20** (2008)285215.

- [19] *Chakraborty, T.; Manaselyan, A.; Barseghyan, M.; Laroze, D.* Controllable continuous evolution of electronic states in a single quantum ring, *Phys. Rev. B* **97**(2018) 041304.
- [20] *O. Ciftja, J. Batle, M. Abdel-Aty, M. A. Hafez, S. Alkhazaleh*, Spatial Entanglement Between Electrons Confined to Rings. *Symmetry* **16**(2024)1662.
- [21] *A. Radu, C. Stan, D. Bejan*. Finite element 3D model of a double quantum ring: effects of electric and laser fields on the interband transition. *New J. Phys.* **25** (2023) 113025.
- [22] *S. Sakiroglu, H. Sari*. *Electric field-induced electronic structure and intersubband transitions of a hydrogen molecular ion in a gaussian-type quantum ring*. *Eur. Phys. J. Plus* **139** (2024) 616.
- [23] *D. Bejan, C. Stan*, Geometry-Tuned Optical Absorption Spectra of the Coupled Quantum Dot–Double Quantum Ring Structure, *Nanomaterials* **14** (2024) 1337.
- [24] *D. Bejan, C. Stan, A. Petrescu-Niță*, Magneto-absorption spectra of laser dressed coupled quantum dot-double quantum ring, *Nanomaterials* **15** (2025) 869.
- [25] *M. E. Mora-Ramos, J. A. Vinasco, A. Radu et al.* Double quantum ring under an intense nonresonant Laser Field: Zeeman and spin-orbit interaction effects. *Cond. Matt.* **8** (2023) 79.
- [26] COMSOL Multiphysics® v. 5.6. www.comsol.com. COMSOL AB, Stockholm, Sweden.
- [27] *D. Bejan, C. Stan*, Aharonov-Bohm oscillations in pseudo-elliptic quantum rings: influence of geometry, eccentricity and electric field, *Eur. Phys. J. Plus* **134** (2019) 127.
- [28] *E. Paspalakis, J. Boviatsis, S. Baskoutas*, Effects of probe field intensity in nonlinear optical processes in asymmetric semiconductor quantum dots. *J. Appl. Phys.* **114** (2013) 153107.